Terahertz echoes reveal the inhomogeneity of aqueous salt solutions

Shalit, Andrey ; Ahmed, Saima ; Savolainen, Janne ; Hamm, Peter

Abstract: The structural and dynamical properties of water are known to be affected by ion solvation. However, a consistent molecular picture that describes how and to what extent ions perturb the water structure is still missing. Here we apply 2D Raman–terahertz spectroscopy to investigate the impact of monatomic cations on the relaxation dynamics of the hydrogen-bond network in aqueous salt solutions. The inherent ability of multidimensional spectroscopy to deconvolute heterogeneous relaxation dynamics is used to reveal the correlation between the inhomogeneity of the collective intermolecular hydrogen-bond modes and the viscosity of a salt solution. Specifically, we demonstrate that the relaxation time along the echo direction t1 = t2 correlates with the capability of a given cation to 'structure' water. Moreover, we provide evidence that the echo originates from the water–water modes, and not the water–cation modes, which implies that cations can structure the hydrogen-bond network to a certain extent.

DOI: https://doi.org/10.1038/nchem.2642

Terahertz Echoes Reveal the Inhomogeneity of Aqueous Salt Solutions

Andrey Shalit, Saima Ahmed, Janne Savolainen, and Peter Hamm
Department of Chemistry, University of Zurich, Winterthurerstrasse 190, CH-8057 Zurich, Switzerland, peter.hamm@chem.uzh.ch
(Dated: September 20, 2016)

The structural and dynamical properties of water are known to be affected by ion solvation. However, a consistent molecular picture describing how and to what extent ions perturb the water structure is still missing. Here we apply two-dimensional Raman-THz spectroscopy to investigate the impact of monatomic cations on the relaxation dynamics of the hydrogen bond network in aqueous salt solutions. The inherent ability of multidimensional spectroscopy to deconvolute heterogeneous relaxation dynamics is used to reveal the correlation between the inhomogeneity of the collective intermolecular hydrogen-bond modes and the viscosity of a salt solution. Specifically, we demonstrate that the relaxation time along the echo direction t_1=t_2 correlates with the capability of a given cation to "structure" water. Moreover, we provide evidence that the echo originates from the water-water modes, and not the water-cation modes, implying that cations can structure the hydrogen-bond network to a certain extent.

Despite significant experimental and theoretical efforts over several decades, the microscopic mechanisms leading to the various anomalous properties of water, whether as neat substance or as a primary biological solvent, are far from being fully understood. The general consensus nowadays is that the ability of water to form complex hydrogen bond networks is primarily responsible for the discrepancies in its various dynamical and thermodynamical properties compared to simple liquids [1, 2]. However, the exact structure of these hydrogen bond networks, the spatial extent to which they persist as well as the relevant time scales are not known. Nevertheless, the language of "water structure" has been widely adopted on a rather empirical level, particularly when attempting to elucidate the effect of ions on the surrounding water molecules upon solvation.

It was first observed by Poiseuille in 1847 [3] that the viscosity of water (η) changes upon solvation of simple inorganic salts in an ion specific manner. Later, the semi-empirical Jones-Dole equation [4]

$$\eta/\eta_w = 1 + Ac^{1/2} + Bc + Dc^2..., \qquad (1)$$

was put forward to quantify this behavior, where η_w is viscosity of neat water and c the ion concentration. Coefficients A and D result from the long-range Coulombic forces and ion pairing, respectively, while B, which depends on ion-water interaction, remained largely empirical up to now [5]. Depending on the sign of the B coefficient, ions are usually categorized as either "structure makers" (B>0) or "structure breakers" (B<0) [6, 7], again without comprehensive molecular picture behind these terms. At least for simple monoatomic ions, the viscosity effect correlates with the charge density, i.e., with increasing charge and decreasing size of an ion the viscosity effect increases. While it is quite clear that solvated ions dramatically affect the hydrogen bond network in their immediate vicinity due to electrostatic interactions, the question remains whether this effect extends beyond the first solvation shell.

The intensive experimental and computational studies including NMR [8], dielectric relaxation [9–11], diffraction methods [12–14], ultrafast vibrational spectroscopies [11, 15–19] and molecular dynamics simulations (MD) [20, 21] over the years resulted in very diverse and in part conflicting interpretations of ion solvation. For example, neutron scattering experiments by Soper and coworkers have indicated an influence of ions on the second peak of the oxygen-oxygen radial distribution function (RDF), which reflects the tetrahedral hydrogen-bond structure of water [13]. However, these experiments revealed no difference when comparing monovalent Na^+ vs. divalent Mg^{2+} cations [14], thus, they do not follow the macroscopic viscosity trend discussed above. On the other hand, ultrafast infrared (IR) measurements of isotope-diluted water (HOD in H_2O) by Bakker and coworkers demonstrated that orientational relaxation of waters beyond the first solvation shell is not affected by ion solvation, even at very high salt concentrations [15]. Later, this claim was somewhat softened when longer range effects were observed for specific combinations of strongly hydrated ions [19]. The seemingly contradicting interpretations might stem from the fact that each of these technique is sensitive only to a specific property of the hydrogen bond network. That is, diffraction methods can capture only the average structure omitting any dynamical aspect, while ultrafast IR spectroscopy, which possesses the necessary time resolution, is capable to measure the hydrogen bond dynamics only indirectly and only very locally by typically monitoring the intramolecular hydroxyl stretch vibration of the water molecule.

A more direct measurement of the effect of salts on the hydrogen bond network was performed by Meech and coworkers [22, 23]. They applied ultrafast heterodyned-detected optical Kerr effect (OKE) spectroscopy to study the influence of hydrated ions on the collective intermolecular modes of water in the low-frequency spectral region below 1000 cm^{-1}. Various Terahertz (THz) absorption [24, 25] and Raman scattering techniques [26, 27] established that the spectral response in this region is

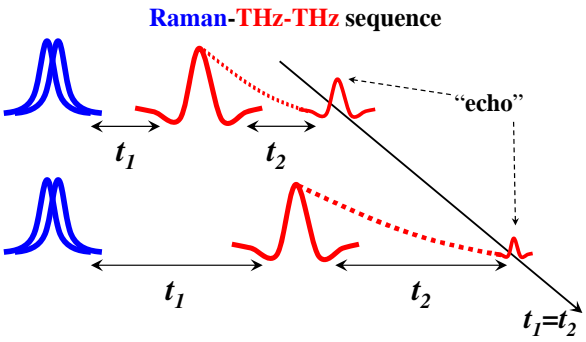

FIG. 1: Raman-THz-THz pulse sequence. The appearance of an echo at t_2=t_1 reflects the ability of the system to rephase the coherence after the second light perturbation.

governed by the water's intermolecular degrees of freedom and consist mainly of three broad peaks around 600 cm^{-1} (hindered rotations), 200 cm^{-1} (hydrogen bond stretch) and 60 cm^{-1} (hydrogen bond bend). The polarization sensitivity as well as time resolution offered by OKE allows one to disentangle the water-ion contribution (isotropic response) from the collective response of the hydrogen bond network (anisotropic response). It has been shown that the decay time of the anisotropic signal correlates with viscosity, where aqueous salt solutions with strongly hydrated ions show significantly slower relaxation dynamics [23]. Nevertheless, OKE spectroscopy as a one dimensional (1D) technique is incapable of providing information regarding the inhomogeneity of the vibrational dynamics [28] that reflects the structural heterogeneity induced by solvated ions.

In order to resolve such an inhomogeneous distribution, a measurement of higher-order correlation functions is required, which is usually achieved by means of multidimensional spectroscopy, where the system is subjected to multiple perturbations [29]. Low-frequency molecular resonances can be probed either directly by THz electromagnetic fields through the dipole moment or indirectly by Raman interaction through a molecular polarizability. Following the advances in generation of strong THz fields [30] required for a non-linear interaction, various multidimensional THz techniques have emerged recently but their applicability is currently limited to semiconductor solids [31] or molecules in the gas phase [32]. To investigate intermolecular collective modes of liquids in the low-frequency range of a few 100 cm^{-1}, Tanimura and Mukamel have proposed 5th-order 2D Raman spectroscopy over 20 years ago [33], however, the realization of that experiment turned out to be exceptionally difficult due to cascading of lower order nonlinear processes [34]. The 5th-order Raman signal could be isolated for certain liquids such as CS_2 or formamide [35–38], but not yet for water due to its very weak Raman cross section. Only very recently, the cascading problem was overcome in a single-beam spectrally controlled technique [39].

Our group has proposed a hybrid method, denoted 2D Raman-THz spectroscopy [40, 41]. While revealing similar information, the new approach is experimentally more feasible than 2D Raman spectroscopy due to the inherent elimination of cascading effects and the large THz cross section of water, and indeed, very recently the first 2D Raman-THz experiment of neat water at ambient conditions has been carried out [42]. In the so-called Raman-THz-THz pulse sequence shown in Fig. 1, two non-resonant field interactions induce a Raman transition and excite an intermolecular vibrational coherence, which quickly dephases due to homogeneous as well as inhomogeneous line broadening. After a time t_1, the system is perturbed a second time by a THz field interaction, and is then read out along t_2 by the emission of a THz field. The amount of inhomogeneity can be monitored through the extent of the signal along the diagonal t_1=t_2. That signal, usually denoted as an "echo", reflects the ability of the system to rephase the coherence after the second perturbation [29].

In the current work, we exploit the unique capabilities of this new spectroscopic tool to investigate how the "structure making" capability of certain cations affects the 2D Raman-THz response. We present a systematic study of a series of aqueous solutions of chloride salts $M^{n+}Cl_n$, where M^{n+} is the cation varied from "structure breaking" (Cs^+, B=-0.047 M^{-1}) to "structure making" (Mg^{2+}, B=0.385 M^{-1}) [5]. The Cl^- anion was kept constant in this series, because its B-coefficient is very close to 0 (B=-0.005 M^{-1}, B-factors of cations and anions are essentially additive) [5]. We restrict our study to simple monatomic cations, because the range of B-coefficients that can be covered is much larger than what would be possible with the monatomic halide anions Cl^- and Br^- [5] (I^- would not be possible due to its low ionisation threshold that leads to dominating THz signals from solvated electrons [43]). We use the same cation concentration of 2 M throughout, which is not an uncommon concentration range for this type of studies [13, 15, 19, 21, 22, 44]. In this concentration range the B-term in Eq. 1 dominates, while ion pairing and clustering, described by the D-term, does not yet play a significant role. We will show that the inhomogeneity of the intermolecular hydrogen bond vibrations, measured via the extent of the "echo" signals along the t_1=t_2 diagonal, increases as the "structure making" property of the cation becomes larger.

I. RESULTS

Figure 2a–d presents a series of 2D Raman-THz signals of 2M aqueous chloride salts solutions with Cs^+ (Fig. 2a), Na^+ (Fig. 2b), Sr^{2+} (Fig. 2c) and Mg^{2+} (Fig. 2d) in an increasing order of water "structure making" capabilities.In our specific experimental layout, the Raman-THz-THz pulse appears in the upper-right quadrant of the 2D response, and the THz-Raman-THz pulse se-

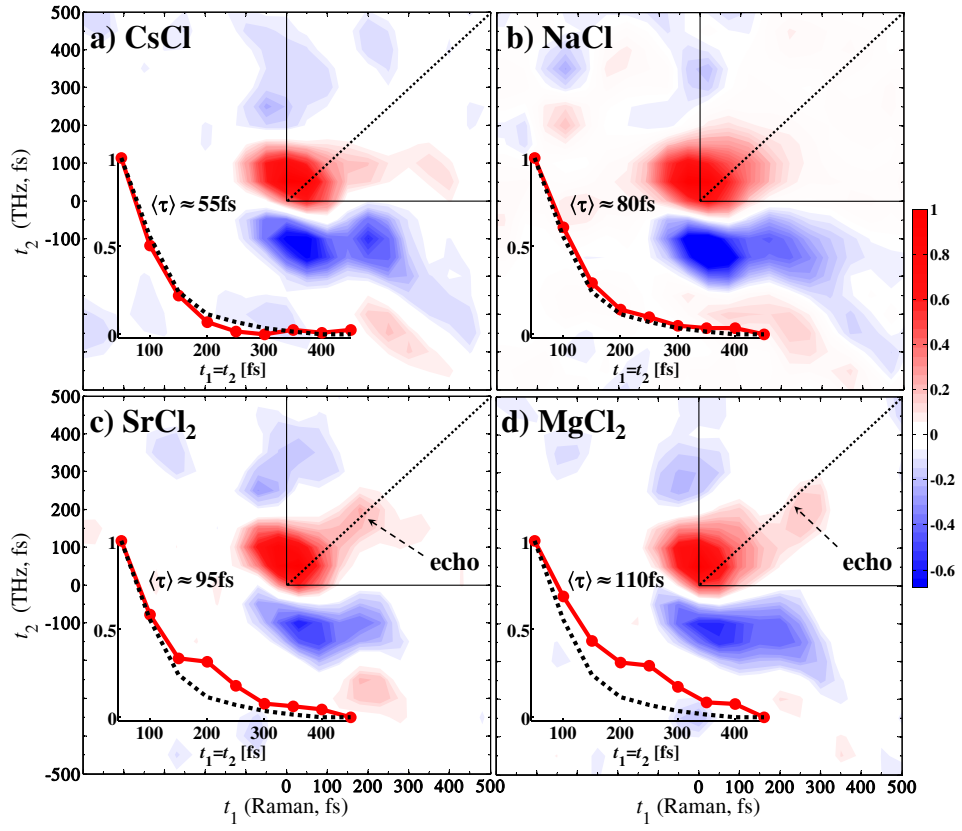

FIG. 2: 2D Raman-THz-THz responses of 2M aqueous salt solutions. Experimental signals for a) CsCl, b) NaCl, c) $SrCl_2$, d) $MgCl_2$. The upper-right quadrant corresponding to the Raman-THz-THz pulse sequence and the main diagonal (dashed line) is indicated. 1D cuts along the t_1=t_2 diagonal for the corresponding salt (red, solid line) and neat water (dashed, black line) are shown in the insets. The 1D and 2D data are normalized to the maximum signal. An increasing structure making ability of the cation manifest itself by an extended relaxation component along the main diagonal.

quence in the upper triange of the upper-left quadrant (the third THz-THz-Raman pulse sequence has recently been implemented by others as well [45]). As has been discussed in our previous publication [42], the molecular response is significantly smeared out by the convolution with the THz and Raman pulses, both having a finite duration, making the interpretation of the observed signal quite difficult. Nevertheless, owing to the shorter duration of the Raman pulse compared to the THz pulse, the Raman-THz-THz pulse sequence, is less susceptible to the contamination from the instrument response function (see instrument response function shown as Fig. 2C of Ref. [42]), and thus will be considered from this point on.

A clear trend between the temporal extent of the diagonal signal in the upper-right quadrant and the *B*-coefficient of the considered cation can be noticed right away. Whereas the 2D Raman-THz response of CsCl in Fig. 2a strongly resembles that of neat water (Fig. S1, Supporting Information), the increase in "structure making" ability of the cation, as in the case of Na^+, is clearly accompanied with slowed down relaxation along the main diagonal t_1=t_2 in the upper-right quadrant (Fig. 2b). This effect becomes much more pronounced for the stronger "structure-modifiers" Sr^{2+} and Mg^{2+}, i.e., for the divalent cations, for which a ridge along the diagonal is formed (Figs. 2c,d).

The insets in Fig. 2 highlight the signals along the diagonal (red solid line) and compare it to that of neat water (black dashed line). Although the latter has been reported before [42], the measurement has been repeated for consistency and is presented in Supplementary Materials (Supplementary Figure 1), where possible sources of small discrepancies in the instrument response functions are discussed as well. For a quantitative analysis, the averaged relaxation time has been calculated for each diagonal cut, defined as $\langle\tau\rangle \equiv \int_{t_0}^{\infty}(\tau - t_0)g(\tau)d\tau / \int_{t_0}^{\infty} g(\tau)d\tau$, where t_0=50 fs represents the peak of the signal. An averaged relaxation time of $\langle\tau\rangle \approx 65 \pm 4$ fs is revealed for neat water, which is the same as the value obtained from our previously published data (see Supplementary Figure 2) [42]. In the case of CsCl, the signal decays somewhat faster with $\langle\tau\rangle \approx 55 \pm 4$ fs, whereas a slower relaxation with $\langle\tau\rangle \approx 80 \pm 7$ fs is obtained for NaCl. The deviations

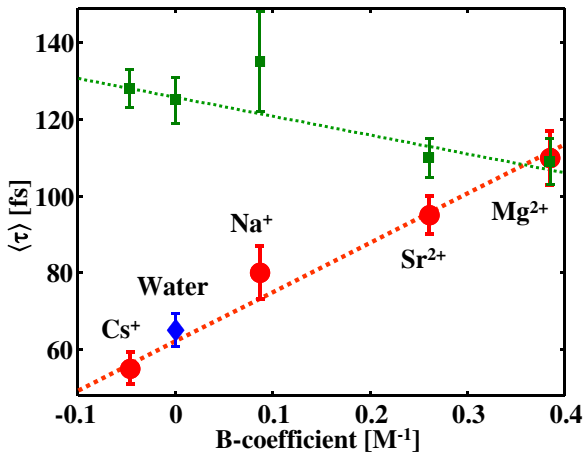

FIG. 3: Averaged relaxation time $\langle\tau\rangle$ as function of B-coefficient of the cation, which has been taken from Ref. [5]. Experimental values for the diagonal decay of aqueous salt solutions are shown as red circles, while the value for neat water is indicated as a blue diamond (assuming a B-coefficient of 0). A linear fit, intersecting at $\langle\tau\rangle$=62 fs for B=0, is depicted. The green squares show the same for the signal decay along the t_1-axis for t_2=-100 fs fixed, which corresponds to the maximum of the blue ridge in the 2D data (see Fig. 2). Error bars (±1 standard deviation) have been estimated by block-averaging.

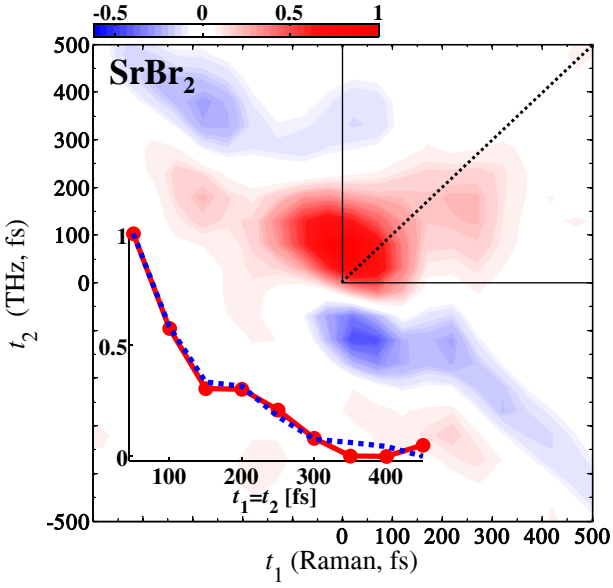

FIG. 4: 2D Raman-THz response of 2M $SrBr_2$ solution. 1D cuts along the t_1=t_2 diagonal for $SrBr_2$ (red solid line) and for $SrCl_2$ taken from Fig. 2c (dashed blue line) are shown in the insets. The relaxation along the diagonal does not depend on the counter anion.

from the neat water signal are much stronger for $SrCl_2$ and $MgCl_2$ with relaxation times of $\langle\tau\rangle\approx 95\pm5$ fs and $\langle\tau\rangle\approx 110\pm7$ fs, respectively. In the latter two cases, an additional oscillatory feature evolves in the echo signal, which can be fitted by a damped oscillator with frequencies $\approx 230\pm20$ cm^{-1} for $SrCl_2$ and $\approx 150\pm15$ cm^{-1} for $MgCl_2$. Fig. 3 (red) shows that the averaged relaxation time along the diagonal correlates perfectly with the B-coefficient of the cation.

II. DISCUSSION

An echo occurs if the memory to rephase persist for a time similar to the free induction decay or longer. In that regard, it is interesting to compare the diagonal decay (Fig. 3, red) with that along the t_1-axes, which is shown in Fig. 3 in green (while we do observe an extended ridge along the t_1-axis, the same is suppressed in the t_2-direction due to the time-derivative occurring in the signal generation process, see Eq. 2 of Ref. [42]). Both decay times approach each other for $MgCl_2$, in which case one is definitely in the regime to call it an echo. Interestingly, the along-the-axis decay shows the opposite trend than the echo decay, i.e., becomes slightly faster for cations with larger B-coefficients. That signal is related to the initial drop of the free-induction in a 1D Raman experiment, hence the speed-up indicates a broader overall (i. e., combined homogeneous and inhomogeneous) linewidth. In the contrary, the echo decay along the diagonal reflects exclusively the homogeneous dephasing of the investigated vibrational modes, thus the data in Fig. 3 present a trend of increasing inhomogeneity with increasing viscosity along the series Cs^+ <Na^+ <Sr^{2+} <Mg^{2+}. The longest echo lifetime we observe, 110 fs for Mg^{2+}, is still fast compared to the typical hydrogen bond lifetime of 1 ps [46–49]. However, in the low-frequency range the collective, intermolecular modes of the hydrogen bond networks involve more than one hydrogen bond, hence, the persistent time of these modes will be shorter.

It is important to stress that there are two possible types of low frequency modes in aqueous salt solutions. That is, in addition to the water-water intermolecular modes, there is a new set of ion-water vibrational modes from the first solvation layer [22, 23, 44, 50]. In the following, we will provide three pieces of evidence that taken together make us believe that the enhanced diagonal feature originates from the intermolecular water-water vibrational modes, and not from ion-water vibrational modes:

- First, the red dashed line in Fig. 3 shows a linear fit through the four salt measurements (red circles). Even though that fit did not include the water value (blue diamond), the latter perfectly falls on the fit with a deviation of only 3 fs. That emphasizes that both experiments, neat water vs. salt solution, measure the inhomogeneity of the same set of vibrational modes, i.e., the intermolecular water-water modes.

- As a second piece of evidence, we compare the frequency of the oscillatory feature in the photon echo signal observed for both Sr^{2+} and Mg^{2+} with what is known from 1D spectroscopy [22, 23, 44, 50]. With regard to water-cation vibrations, Havenith and coworkers [44] have identified distinct vibrational bands for both $SrCl_2$ and $MgCl_2$ in linear THz absorption spectra, however, with opposite frequency ordering ($\approx$100 cm^{-1} for $SrCl_2$ vs. $\approx$200 cm^{-1} for $MgCl_2$, which in essence simply reflects the much larger mass of Sr^{2+}) as compared to our observation ($\approx$230 cm^{-1} for $SrCl_2$ vs. $\approx$150 cm^{-1} for $MgCl_2$, which can be discriminated within the error bars of the fitted beat frequencies).

- Finally, we substituted the Cl^- anion by Br^- while keeping the same strong "structure-making" Sr^{2+} cation (Fig. 4), in order to also test possible water-anion vibrations. Regarding 1D spectroscopy, conflicting results can be found in the literature with frequencies that seem to depend on the spectroscopic method (THz absorption [44, 50] vs. Raman [22, 23], indicating a non-coincident effect from delocalized modes [51]), or on the charge of the cation (monovalent [22, 23, 44] vs. divalent [50]). However, in any case, the frequency of the anion-water vibration depends on the nature of the ion, in some cases as extremely as $\approx$200 cm^{-1} for Cl^- to $\approx$50 cm^{-1} for Br^- [44], again following the mass of the anion. In contrast, Fig. 4 shows that the 2D Raman-THz responses of both $SrCl_2$ and $SrBr_2$ are virtually the same with a significant prolongation of the diagonal signal and a profound oscillatory contribution in the echo signal with a frequency of $\approx$230 cm^{-1} in both cases.

Hence, the echo signal does not seem to stem from water-ion vibrations. While a detailed explanation of the oscillatory feature in the echo signal is currently missing, it is very suggestive to see that its frequency falls into the broad hydrogen bond stretch vibration of liquid water, which is centered around $\approx$200 cm^{-1}.

A full understanding of the 2D Raman-THz response will require extensive theoretical and simulation work. Such work has indeed identified echo features for neat water [41, 52–55], however, in contrary to our observation, only for the THz-Raman-THz pulse sequence, which would lie in the upper-left quadrant along $-2t_1 = t_2$ in our representation of the data (i.e., along the blue line of Fig. S1). Tanimura and coworkers have explained that effect by the larger anharmonicity of the Raman interaction, resulting in a more efficient two-quantum transition needed to obtain an "inversion of coherence" that eventually results in rephasing [56]. However, the simulated echo features are very short-lived and likely originate from the librational modes of water that are completely suppressed in our experiment due to the limited time resolution. The only simulation work we are aware of that includes ions is by Zhuang and coworkers [57], who saw a slight prolongation of the main peak around $t_1 = t_2 = 0$ in the Raman-THz-THz echo direction for a 3.5M $MgCl_2$ solution. Also that effect is extremely short-lived and would not be observable with our current time resolution. Unfortunately, the limited simulation time of Ref. [57] does not allow for any conclusions on slower dynamics as the one observed here (as a general remark, the convergence of the multi-timepoint correlation functions needed to calculate a 2D Raman-THz signal from MD simulations becomes exponentially more computer-time expensive when longer times t_1 and t_2 are considered).

It has been shown in Ref. [58] that the 2D Raman-THz signal of neat water is an extremely sensitive probe of the level of accuracy with which polarizability of a water model is described, and that is expected to become even more relevant once the charge of an ion is introduced. From the water models considered in Ref. [58], by far the best agreement with the experimental 2D Raman-THz response was achieved with the TL4P water model recently put forward by Tavan and coworkers [59]. It is a rigid 4-point model that features a Gaussian shaped inducible dipole, which allows one to realize a transferable model that describes both the gas and the solution phase dipole moment and polarizability correctly, avoiding the usual problems of the polarization catastrophe. It will be interesting to see whether ions parametrized consistently to the TL4P water model can reproduce the experimental results reported here.

III. CONCLUSION

In conclusion, we have identified an extended relaxation component along the t_1=t_2 direction by comparing the 2D Raman-THz response of neat water with that of a series of chloride salts. As the "structure making" ability of the cation increases, the echo feature becomes longer and evolves an oscillatory contribution. As in the case of the conceptually similar 2D Raman spectroscopy, such a echo reflects the amount of inhomogeneity of the corresponding degrees of freedom. The echo decay time correlates perfectly with the Jones-Dole B-coefficient. Even though a correlation does not necessarily imply causation, this observation still connects a macroscopic observable (viscosity) to the microscopic heterogeneity of hydrogen bond networks. We find the slight speed up of the echo decay for Cs^+ rather remarkable, as to the best of our knowledge, such an acceleration has not been observed before by any other spectroscopic technique. Moreover, we provide evidence that the enhanced structural heterogeneities do not originate from water-ion vibrations but are related to water-water modes. This observation implies structuring effects on the hydrogen-bond networks, thus confirming the empirically used concept of "structure makers" or "structure breakers" on a molecular level.

Given the extraordinary sensitivity of the method to detect the polarizability of the various molecular con-

stituents [58], we believe that these experiments are the most decisive experiments of ion solvation as to date, despite the fact that the full information currently cannot be retrieved. A more thorough interpretation of the experimental results will require massive support from theory, and we hope that our current interpretation will serve as a working hypothesis for theoretical work to come.

Acknowledgments

We thank Philip J. M. Johnson for many other insightful discussions. The work has been supported by the Swiss National Science Foundation (SNF) through the NCCR MUST.

Author contributions

A.S., J.S and P.H. conceived and designed the experiments. A.S. and S.A. performed the experiments. A.S analysed the data. A.S. and P.H. co-wrote the paper. All authors discussed the results and commented on the manuscript.

Additional information

Correspondence and requests for materials should be addressed to A.S. and P.H.

IV. METHODS

The experimental setup for 2D Raman-THz spectroscopy was described in details elsewhere [42]. Briefly, a train of short (∼100 fs) 800 nm pulses with bandwidth of 300 cm^{-1} (∼9 THz) delivered from a 5 kHz amplified Ti:sapphire laser was split into three beams. The first beam, denoted as Raman pump, was used to excite a vibrational coherence in the sample through two field interactions. Before hitting the sample, the Raman pump pulses passed through an optical delay stage defining time t_1. Their energy were varied from 200 μJ for neat water (Fig. 1S) down to 40 μJ for $SrBr_2$ in order to avoid the otherwise strong contributions from a hydrated electron generated by multi-photon processes [43]. The second beam was used to generate short THz pulses by means of optical rectification, which were focused onto the sample by means of an elliptical mirror, and the third beam was used to detect the transmitted THz pulses by electro-optic sampling. Before hitting the detection crystal, the detection beam was passed through another delay stage defining time t_2. For both THz generation and detection, a 100 μm thick (110) GaP crystal was used, which gave higher bandwidth as the more common ZnTe crystal and very clean half-cycle pulses with essentially no ringing. The pulse duration of the THz pulse was ≈140 fs, peaking at ∼1.4 THz and extending to ≈7 THz, which is sufficient to excite and probe the water's hydrogen bond stretch band at ≈200 cm^{-1}. The foci of both THz and Raman pulses were matched with ≈250 μm on a ≈40 μm thick wire-guided, gravity-driven jet to avoid any undesired extra signals from windows. Each measurement consists of ≈100 individual 2D-scans, each scanning t_1 and t_2 on a 50 fs grid. The total averaging time of each measurement amounted to ≈60 h. All measurement were performed at room temperature.

[1] Debenedetti, P. G. Supercooled and glassy water. *J. Phys.- Condens Matter* **15**, R1669 (2003).

[2] Stanley, H. E. *et al.* Liquid polyamorphism: Possible relation to the anomalous behaviour of water. *Eur. Phys. J. Special Topics* **161**, 1–17 (2008).

[3] Sutera, S. P. & Skalak, R. The history of Poiseuille's law. *Annu. Rev. Fluid Mech.* **25**, 1–20 (1993).

[4] Jones, G. & Dole, M. The viscosity of aqueous solutions of strong electrolytes with special reference to barium chloride. *J. Am. Chem. Soc.* **51**, 2950–2964 (1929).

[5] Jenkins, H. D. B. & Marcus, Y. Viscosity B-coefficients of ions in solution. *Chem. Rev.* **95**, 2695–2724 (1995).

[6] Gurney, R. W. *Ionic Processes In Solution* (McGrawHill,, New York, 1953).

[7] Frank, H. S. & Wen, W.-Y. Ion-solvent interaction. Structural aspects of ion-solvent interaction in aqueous solutions: a suggested picture of water structure. *Discuss. Faraday Soc.* **24**, 133–140 (1957).

[8] Struis, R. P. W. J., Bleijser, J. D. & Leyte, J. C. $^{25}Mg^{2+}$ and $^{35}Cl^{-}$ quadrupolar relaxation in aqueous $MgCl_2$ solutions at 25 ° C. 2. Relaxation at finite $MgCl_2$ concentrations. *J. Phys. Chem.* **93**, 7943–7952 (1989).

[9] Buchner, R., Chen, T. & Hefter, G. Complexity in "simple" electrolyte solutions:Ion pairing in $MgSO_4$(aq). *J. Phys. Chem. B* **108**, 2365–2375 (2004).

[10] Wachter, W., Kunz, W., Buchner, R. & Hefter, G. Is there an anionic Hofmeister effect on water dynamics? Dielectric spectroscopy of aqueous solutions of NaBr, NaI, $NaNO_3$, $NaClo_4$, and NaSCN. *J. Phys. Chem. A* **109**, 8675–8683 (2005).

[11] Turton, D. A., Hunger, J., Hefter, G., Buchner, R. & Wynne, K. Glasslike behavior in aqueous electrolyte solutions. *J. Chem. Phys.* **128**, 161102 (2008).

[12] Näslund, L.-A. *et al.* X-ray absorption spectroscopy study of the hydrogen bond network in the bulk water of aqueous solutions. *J. Phys. Chem. A* **109**, 5995–6002

(2005).

[13] Mancinelli, R., Botti, A., Bruni, F., Ricci, M. A. & Soper, A. K. Perturbation of water structure due to monovalent ions in solution. *Phys. Chem. Chem. Phys.* **9**, 2959–2967 (2007).

[14] Bruni, F., Imberti, S., Mancinelli, R. & Ricci, M. A. Aqueous solutions of divalent chlorides: Ions hydration shell and water structure. *J. Chem. Phys.* **136**, 064520 (2012).

[15] Omta, A. W., Kropman, M. F., Woutersen, S. & Bakker, H. J. Negligible effect of ions on the hydrogen-bond structure in liquid water. *Science* **301**, 347–349 (2003).

[16] Kropman, M. F. & Bakker, H. J. Effect of ions on the vibrational relaxation of liquid water. *J. Am. Chem. Soc.* **126**, 9135–9141 (2004).

[17] Park, S. & Fayer, M. D. Hydrogen bond dynamics in aqueous NaBr solutions. *Proc. Natl Acad. Sci. USA* **104**, 16731–16738 (2007).

[18] Moilanen, D. E., Wong, D., Rosenfeld, D. E., Fenn, E. E. & Fayer, M. D. Ionwater hydrogen-bond switching observed with 2D IR vibrational echo chemical exchange spectroscopy. *Proc. Natl Acad. Sci. USA* **106**, 375–380 (2009).

[19] Tielrooij, K. J., Garcia-Araez, N., Bonn, M. & Bakker, H. J. Cooperativity in ion hydration. *Science* **328**, 1006–1009 (2010).

[20] Stirnemann, G., Wernersson, E., Jungwirth, P. & Laage, D. Mechanisms of acceleration and retardation of water dynamics by ions. *J. Am. Chem. Soc.* **135**, 11824–11831 (2013).

[21] Zhang, R. & Zhuang, W. Cation effect in the ionic solution optical Kerr effect measurements: A simulation study. *J. Chem. Phys.* **140**, 054507 (2014).

[22] Heisler, I. A. & Meech, S. R. Low-frequency modes of aqueous alkali halide solutions: Glimpsing the hydrogen bonding vibration. *Science* **327**, 857–860 (2010).

[23] Heisler, I. A., Mazur, K. & Meech, S. R. Low-frequency modes of aqueous alkali halide solutions: An ultrafast optical Kerr effect study. *J. Phys. Chem. B.* **115**, 1863–1873 (2011).

[24] Bertie, J. E. & Lan, Z. Infrared intensities of liquids XX: The intensity of the OH stretching band of liquid water revisited, and the best current values of the optical constants of H_2O(l) at 25 ° C between 15,000 and 1 cm^{-1}. *Appl. Spectrosc.* **50**, 1047–1057 (1996).

[25] Mazur, K., Heisler, I. A. & Meech, S. R. THz spectra and dynamics of aqueous solutions studied by the ultrafast optical Kerr effect. *J. Phys. Chem. B* **115**, 2563–2573 (2011).

[26] Torre, R., Bartolini, P. & Righini, R. Structural relaxation in supercooled water by time-resolved spectroscopy. *Nature* **428**, 296–299 (2004).

[27] Fukasawa, T. *et al.* Relation between dielectric and low-frequency Raman spectra of hydrogen-bond liquids. *Phys. Rev. Lett.* **95**, 197802 (2005).

[28] Loring, R. F. & Mukamel, S. Selectivity in coherent transient Raman measurements of vibrational dephasing in liquids. *J. Chem. Phys.* **83**, 2116–2128 (1985).

[29] Hamm, P. & Zanni, M. T. *Concepts and methods of 2D infrared spectrsocopy* (Cambridge University Press, Cambridge, 2011).

[30] Hwang, H. Y. *et al.* A review of non-linear terahertz spectroscopy with ultrashort tabletop-laser pulses. *J. Mod. Opt.* **62**, 1447–1479 (2015).

[31] Kuehn, W. *et al.* Strong correlation of electronic and lattice excitations in GaAs/AlGaAs semiconductor quantum wells revealed by two-dimensional terahertz spectroscopy. *Phys. Rev. Lett.* **107**, 067401 (2011).

[32] Fleischer, S., Field, R. W. & Nelson, K. A. Commensurate two-quantum coherences induced by time-delayed THz fields. *Phys. Rev. Lett.* **109**, 123603 (2012).

[33] Tanimura, Y. & Mukamel, S. Two-dimensional femtosecond vibrational spectroscopy of liquids. *J. Chem. Phys.* **99**, 9496–9511 (1993).

[34] Blank, D. A., Kaufman, L. J. & Fleming, G. R. Fifth-order two-dimensional Raman spectra of CS_2 are dominated by third-order cascades. *J. Chem. Phys.* **111**, 3105–3114 (1999).

[35] Golonzka, O., Demirdöven, N., Khalil, M. & Tokmakoff, A. Separation of cascaded and direct fifth-order Raman signals using phase-sensitive intrinsic heterodyne detection. *J. Chem. Phys.* **113**, 9893–9896 (2000).

[36] Kaufman, L. J., Heo, J., Ziegler, L. D. & Fleming, G. R. Heterodyne-detected fifth-order nonresonant Raman scattering from room temperature CS_2. *Phys. Rev. Lett.* **88**, 207402 (2002).

[37] Kubarych, K. J., Milne, C. J. & Miller, R. J. D. Fifth-order two-dimensional Raman spectroscopy: a new direct probe of the liquid state. *Int. Rev. Phys. Chem.* **22**, 497–532 (2003).

[38] Li, Y. L., Huang, L., Miller, R. J. D., Hasegawa, T. & Tanimura, Y. Two-dimensional fifth-order Raman spectroscopy of liquid formamide: Experiment and theory. *J. Chem. Phys.* **128**, 234507 (2008).

[39] Frostig, H., Bayer, T., Dudovic, N., Eldar, Y. C. & Silberberg, Y. Single-beam spectrally controlled two-dimensional Raman spectroscopy. *Nature Photon.* **9**, 339–343 (2015).

[40] Hamm, P. & Savolainen, J. Two-dimensional-Raman-terahertz spectroscopy of water: Theory. *J. Chem. Phys.* **136**, 094516 (2012).

[41] Hamm, P., Savolainen, J., Ono, J. & Tanimura, Y. Note: Inverted time-ordering in two-dimensional-Raman-terahertz spectroscopy of water. *J. Chem. Phys.* **136**, 236101 (2012).

[42] Savolainen, J., Ahmed, S. & Hamm, P. Two-dimensional Raman-terahertz spectroscopy of water. *Proc. Natl Acad. Sci. USA* **110**, 20402–20407 (2013).

[43] Savolainen, J., Uhlig, F., Ahmed, S., Hamm, P. & Jungwirth, P. Direct observation of the collapse of the delocalized excess electron in water. *Nature Chem.* **6**, 697–701 (2014).

[44] Funkner, S. *et al.* Watching the low-frequency motions in aqueous salt solutions: The terahertz vibrational signatures of hydrated ions. *J. Am. Chem. Soc.* **134**, 1030–1035 (2012).

[45] Finneran, I. A., Welsch, R., Allodi, M. A., Miller III, T. F. & Blake, G. A. Coherent two-dimensional terahertz-terahertz-Raman spectroscopy. *Proc. Natl. Acad. Sci. USA* **113**, 6857–6861 (2016).

[46] Asbury, J. B. *et al.* Dynamics of water probed with vibrational echo correlation spectroscopy. *J. Chem. Phys.* **121**, 12431–12446 (2004).

[47] Yeremenko, S., Pshenichnikov, M. S. & Wiersma, D. A. Hydrogen-bond dynamics in water explored by heterodyne-detected photon echo. *Chem. Phys. Lett.* **369**, 107–113 (2003).

[48] Cowan, M. L. *et al.* Ultrafast memory loss and energy

redistribution in the hydrogen bond network of liquid H_2O. *Nature* **434**, 199–202 (2005).

[49] Eaves, J. D. *et al.* Hydrogen bonds in liquid water are broken only fleetingly. *Proc. Natl. Acad. Sci. USA* **102**, 13019–13022 (2005).

[50] Schmidt, D. A. *et al.* Rattling in the cage: Ions as probes of sub-picosecond water network dynamics. *J. Am. Chem. Soc.* **131**, 18512–18517 (2009).

[51] Torii, H. Ultrafast anisotropy decay of coherent excitations and the non-coincidence effect for delocalized vibrational modes in liquids. *Chem. Phys. Lett.* **323**, 382–388 (2000).

[52] Ito, H., Hasegawa, T. & Tanimura, Y. Calculating two-dimensional THz-Raman-THz and Raman-THz-THz signals for various molecular liquids: The samplers. *J. Chem. Phys.* **141**, 124503 (2014).

[53] Ito, H., Jo, J.-Y. & Tanimura, Y. Notes on simulating two-dimensional raman and terahertz-Raman signals with a full molecular dynamics simulation approach. *Struct. Dyn.* **2**, 054102 (2015).

[54] Ikeda, T., Ito, H. & Tanimura, Y. Analysis of 2D THz-Raman spectroscopy using a non-Markovian Brownian oscillator model with nonlinear system-bath interactions. *J. Chem. Phys.* **142**, 212421 (2015).

[55] Ito, H. & Tanimura, Y. Simulating two-dimensional infrared-Raman and Raman spectroscopies for intermolecular and intramolecular modes of liquid water. *J. Chem. Phys.* **144**, 074201 (2016).

[56] Fourkas, J. T. Multidimensional Raman spectroscopies. *Adv. Chem. Phys.* **117**, 235–273 (2001).

[57] Pan, Z. *et al.* Low frequency 2D Raman-THz spectroscopy of ionic solution: A simulation study. *J. Chem. Phys.* **142**, 212419 (2015).

[58] Hamm, P. 2D-Raman-THz spectroscopy: A sensitive test of polarizable water models. *J. Chem. Phys.* **141**, 184201 (2014).

[59] Tröster, P., Lorenzen, K., Schwörer, M. & Tavan, P. Polarizable water nodels from mixed computational and empirical optimization. *J. Phys. Chem. B* **117**, 9486–9500 (2013).